Longitudinal and Transverse Cross Sections in the ^{1}H$(e, e'K^+)\Lambda$ Reaction

G. Niculescu,[1] R. M. Mohring,[2] P. Gueye,[1] D. Abbott,[3] A. Ahmidouch,[1,4] Ts. A. Amatuni,[5] P. Ambrozewicz,[6] T. Angelescu,[7] C. S. Armstrong,[8] K. Assamagan,[1] S. Avery,[1] K. Bailey,[9] O. K. Baker,[1,3] K. Beard,[1] S. Beedoe,[10] E. Beise,[2] H. Breuer,[2] R. Carlini,[3] J. Cha,[1] C. C. Chang,[2] N. Chant,[2] E. Cisbani,[12] G. Collins,[2] W. Cummings,[9] S. Danagoulian,[10] R. De Leo,[12] F. Duncan,[2] J. Dunne,[3] D. Dutta,[13] T. Eden,[1] R. Ent,[3] L. Eyraud,[14] L. Ewell,[2] M. Finn,[8] T. Fortune,[15] V. Frolov,[16] S. Frullani,[12] C. Furget,[14] F. Garibaldi,[12] D. Gaskell,[17] D. F. Geesaman,[9] K. K. Gustafsson,[2] J.-O. Hansen,[9] M. Harvey,[1] W. Hinton,[1] E. Hungerford,[18] M. Iodice,[12] C. Jackson,[10] C. Keppel,[1,3] W. Kim,[19] K. Kino,[20] D. Koltenuk,[15] S. Kox,[14] L. Kramer,[21] T. Leone,[12] G. Lolos,[12] A. Lung,[2] D. Mack,[3] R. Madey,[1,4] M. Maeda,[20] S. Majewski,[3] P. Markowitz,[21] C. J. Martoff,[6] D. Meekins,[8] A. Mihul,[7] J. Mitchell,[3] H. Mkrtchyan,[5] S. Mtingwa,[10] I. Niculescu,[1] R. Perrino,[12] D. Potterveld,[9] J. W. Price,[16] B. A. Raue,[21] J.-S. Real,[14] J. Reinhold,[9] P. Roos,[2] T. Saito,[20] G. Savage,[1] R. Sawafta,[10] R. Segel,[13] S. Stepanyan,[5] P. Stoler,[16] V. Tadevosian,[5] L. Tang,[1,3] L. Teodorescu,[7] T. Terasawa,[20] H. Tsubota,[20] G. M. Urciuoli,[12] J. Volmer,[11] W. Vulcan,[3] P. Welch,[17] R. Williams,[1] S. Wood,[3] C. Yan,[3] and B. Zeidman[9]

[1]*Hampton University, Hampton, Virginia 23668*
[2]*University of Maryland, College Park, Maryland 20742*
[3]*Thomas Jefferson National Accelerator Facility, Newport News, Virginia 23606*
[4]*Kent State University, Kent, Ohio 44242*
[5]*Yerevan Physics Institute, Yerevan, Armenia 375306*
[6]*Temple University, Philadelphia, Pennsylvania 19122*
[7]*Bucharest University, Bucharest, Romania R76900*
[8]*College of William and Mary, Williamsburg, Virginia 23187*
[9]*Argonne National Laboratory, Argonne, Illinois 60439*
[10]*North Carolina A & T State University, Greensboro, North Carolina 27411*
[11]*Free University, Amsterdam, The Netherlands 1081*
[12]*Physics Laboratory, Istituto Superiore di Sanitá and INFN-Sezione Sanitá, Rome, Italy I-00161*
[13]*Northwestern University, Evanston, Illinois 60201*
[14]*ISN, Grenoble, France 38026*
[15]*University of Pennsylvania, Philadelphia, Pennsylvania 19104*
[16]*Rensselaer Polytechnic Institute, Troy, New York 12180*
[17]*Oregon State University, Corvallis, Oregon 97331*
[18]*University of Houston, Houston, Texas 77204*
[19]*Kyungpook National University, Taegu, Republic of Korea*
[20]*Tohoku University, Sendai 982, Japan*
[21]*Florida International University, Miami, Florida 33199*

(Received 27 March 1998)

The ^{1}H$(e, e'K^+)\Lambda$ reaction was studied as a function of the squared four-momentum transfer, Q^2, and the virtual photon polarization, ε. For each of four Q^2 settings, 0.52, 0.75, 1.00, and 2.00 $(\mathrm{GeV}/c)^2$, the longitudinal and transverse virtual photon cross sections were extracted in measurements at three virtual photon polarizations. The Q^2 dependence of the σ_L/σ_T ratio differs significantly from current theoretical predictions. This, combined with the precision of the measurement, implies a need for revision of existing calculations. [S0031-9007(98)06954-3]

PACS numbers: 25.30.Rw, 13.40.Gp, 14.40.Aq

Flavor degrees of freedom provide qualitatively new tests of our understanding of baryon and meson structure. The electromagnetic production of kaons is important for further progress in many fields and subfields of physics such as hypernuclear production and spectroscopy (providing information complementary to that from hadronic reactions such as (K, π), (π, K), and $(p, p'K)$ [1,2]), and some aspects of QCD model building (the (γ, K) and the $(e, e'K)$ reactions are important for an improved understanding of the basic coupling constants needed in various nucleon-meson and quark models [3]) to name only a few. The use of virtual photons (electroproduction) as opposed to real photons (photoproduction) offers access to a much richer body of information because both the virtual photon mass and polarization can be varied independently [4].

This Letter is a report on the first results of a study of associated kaon electroproduction on hydrogen using the medium-energy, high-intensity, electron beam at the Jefferson Laboratory (formerly CEBAF). The excellent beam qualities of the CEBAF accelerator combined with precision magnetic spectrometers allowed a detailed

investigation of the reaction with high systematic and statistical precision, whereas the only prior measurement [5] provided virtually no constraints for the available theories.

Experiment E93-018 was among the first experiments performed in experimental HALL C at Jefferson Lab utilizing the 100% duty factor electron beam. The beam energy was varied between 2.445 and 4.045 GeV with a beam current between 10 and 30 μA. The beam current was measured (to 1% accuracy) with two resonant cavities and a parametric current transformer. Tungsten collimators (2 in. thick) with large octagonal appertures were used to define the solid angle of each spectrometer. The target was a 4.36 ± 0.01 cm liquid-hydrogen cell with a proton abundancy of 99.8%. The background from the beam interaction with the aluminum walls of the target was measured separately using a replica of the (empty) target cell. The scattered electrons were detected in the High Momentum Spectrometer (HMS, momentum acceptance $\pm 10\%$, solid angle ~ 6.7 msr) in coincidence with the kaons detected in the Short Orbit Spectrometer (SOS, momentum acceptance $\pm 20\%$, solid angle ~ 7.5 msr). The detector stack in each spectrometer had four segmented-plastic-scintillator arrays used for trigger formation, time-of-flight (TOF), and energy loss information. Two six-plane multiwire planar drift chambers were used to perform track reconstruction in each spectrometer. Gas threshold Čerenkov counters and segmented lead-glass shower counter arrays provided the signals needed for electron identification.

For the specific purpose of kaon identification, the hadron arm was outfitted with a silica aerogel ($n = 1.034$) detector for K^+/π^+ discrimination and an array of Lucite total internal reflection Čerenkov counters ($n = 1.49$), for K^+/p discrimination.

Recorded for each run were all electron-hadron coincidence events and prescaled electron and hadron single events. Typical momentum resolution achieved with this system was $0.15\%(\sigma)$, while the target angle resolution for each spectrometer was approximately 2–3 mr in both the horizontal and vertical directions. The time resolution of the hodoscope scintillators varied between 110 and 130 ps, allowing for a resolution in particle velocity, β, of $\Delta\beta = 0.018$. The aerogel and Lucite detectors yielded over 14 photoelectrons (on average) for pions and protons, respectively, resulting in π^+/K^+ and p/K^+ separation of better than 100/1 each. When combined with the time-of-flight information, π^+/K^+ and p/K^+ separations of better than 1 part in 800 were achieved. This was more than adequate for good kaon identification in all of the kinematic settings.

To verify the accuracy for the spectrometer acceptance, reconstruction efficiency, dead time corrections as well as the radiative correction procedure, $^1\mathrm{H}(e, e')$ elastic data (measured in both HMS and SOS) were compared with Monte Carlo simulations which included the spectrometer-detector acceptance model and best available parametrizations for the proton magnetic (electric) form factor G_{Mp} (G_{Ep}) [6]. The absolute normalization of the hydrogen cross section agreed with the simulation within 1.5%.

At each kinematic setting, data were partitioned into several runs; the run-to-run variation of various quantities (i.e., dead time, efficiency, etc.) was used as a consistency check. The variations found contribute insignificantly to the systematic uncertainty quoted below.

Figure 1 shows a typical electron-kaon coincidence timing spectrum. The true (real) coincidence peak is defined well, as are the random (accidental) coincidence peaks corresponding to the 499 MHz microstructure of Jefferson Lab's electron beam. The real-to-random ratio is typically 10 to 1 or better for all kinematic settings. Information from the true coincident kaons was used to calculate the missing mass spectrum. Two peaks, identified clearly in Fig. 2, correspond to the masses of Λ (1115) and Σ^0 (1192), respectively. Because of kinematical restrictions in this experiment, the production of higher mass hyperons is forbidden. Subtraction of random coincidence events and target wall contributions yields a clean missing mass spectrum with virtually no events below the Λ threshold. For the purpose of this work, all events with a missing mass value between 1.1 and 1.175 GeV were accepted as valid $e + p \rightarrow e' + K^+ + \Lambda$ coincidence events and used in subsequent calculations.

In the one-photon exchange approximation, the cross section for the scattering of an electron from a hydrogen target, where none of the initial or final spins are detected, can be reduced, in parallel kinematics [7] (appropriate for our experimental setup), to

$$\frac{d^5\sigma}{dE_{e'}d\Omega_{e'}d\Omega_{K^+}} = \Gamma\left(\frac{d\sigma}{d\Omega_{K^+}}\right)^{\mathrm{CM}} = \Gamma(\sigma_T + \varepsilon\sigma_L), \tag{1}$$

where Γ is the virtual photon flux, σ_T is the unpolarized (transverse) cross section, σ_L is the longitudinal cross section, $\Omega_{e'}$ is the scattered electron solid angle, Ω_{K^+} is the kaon solid angle, $E_{e'}$ is the scattered electron energy, and ε is the virtual photon polarization.

The quantities σ_T and σ_L, which can be separated by varying ε with measurements at different beam energies, completely describe the parallel kinematics cross section behavior. Generally they are functions of the kinematic

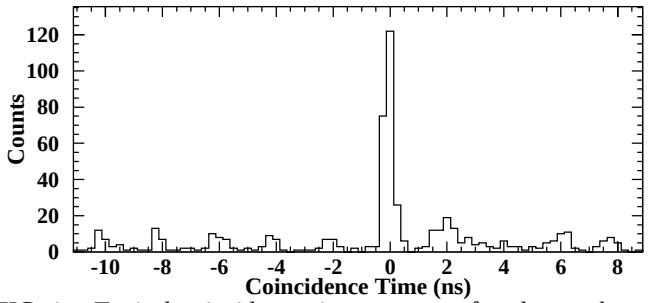

FIG. 1. Typical coincidence time spectrum for electron-kaon coincidences at $Q^2 = 0.52$ (GeV/c)^2.

variables Q^2, the squared four-momentum of the virtual photon, the total energy of the photon-proton system W, and $t = (q - K)^2$, the squared four-momentum transfer between the photon and the kaon. Here q and K denote the four-momenta of the virtual photon and kaon, respectively.

For each kinematic setting, the sample of coincident $e + p \rightarrow e' + K^+ + \Lambda$ events was used to compute the laboratory cross section. Then from Eq. (1), the center-of-mass (CM) cross section $(d\sigma/d\Omega_{K^+})^{\mathrm{CM}}$ was computed (Fig. 3). The uncertainties in these kaon electroproduction cross sections are at the same level or smaller than those in the existing world data set [8–10]. In order to facilitate comparison of data at different values of W and t, all data were scaled to $W = 2.15$ GeV as outlined in Refs. [9,10]. For the cases where more than one ε setting was measured, only the highest value of the cross section is quoted for comparison with older data sets.

The systematic uncertainty assigned to these absolute cross sections is $\sim$5% and is dominated by the uncertainties in acceptance ($\sim$3%) and kaon survival probability (3%); however, the point-to-point random uncertainties, which are the ones relevant for the L-T separation, are smaller because some of the larger overall systematic contributions (such as survival probability, kaon absorption, etc.) are correlated strongly between various ε settings. The point-to-point random uncertainties are at the (2.1–3.0)% level. The statistical uncertainty varied between 0.8% and 2.0% (depending on kinematical setting). Using these values the uncertainty in the σ_L/σ_T ratio (subsequently referred to as "R") is 17% to 45%. These uncertainties are substantially smaller than errors of the only previous R determination [5].

In Fig. 4, the unseparated cross section at each Q^2 is shown as a function of ε together with the best least-squares fit for σ_T and σ_L. Table I presents the summary of the extracted transverse and longitudinal cross sections, the ratio R, as well as their associated uncertainties.

In Fig. 5, the calculated values of R from this experiment are compared with the only other existing data [5]; the two sets of measurements agree reasonably well, although in order to properly show the uncertainties of the previous measurement, the scale in R had to be extended to unphysical negative values.

Two theoretical predictions for σ_L/σ_T, by Williams, Ji, and Cotanch [4] (WJC), and the Saclay-Lyon model described in [11] are included in Fig. 5. Both calculations use phenomenological fits of previous world data sets to extract coupling constants and relevant form factors. The estimated uncertainty in these quantities is indicated by the height of the shaded areas. Both theoretical models predict that the ratio R increases with momentum transfer whereas our data indicate a flat behavior over this range of Q^2 for the given kinematic settings. This discrepancy may be partially explained by a difference between the true kaon electromagnetic form factor and its parametrization, as used in the models. In this kinematic range for Λ production, the data support the existence of a large longitudinal component to the kaon electroproduction cross section which is expected to be dominated by kaon exchange. In general, the L-T current separation is sensitive to the prescription for establishing current conservation in electroproduction models, especially the combination of the non-gauge-invariant terms involving the electric proton and kaon form factors. The precision of the present data indicate that existing prescriptions for the production of even the simplest hadronic system with strangeness are inadequate. This shows a need for revision of the existing kaon electroproduction models and will constrain future models.

The first results from measurements of elementary kaon electroproduction cross sections performed during experiment E93-018 are reported. The center-of-mass cross sections reported here for the reaction $e + p \rightarrow e' + K^+ + \Lambda$

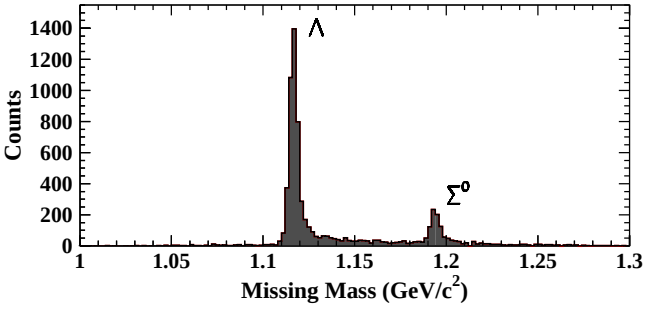

FIG. 2. Missing mass spectrum for the ^{1}H$(e, e'K^+)$ reaction after subtracting random coincidences and target wall contributions. Because no radiative corrections were performed here, radiative tails are seen projecting towards higher missing mass values.

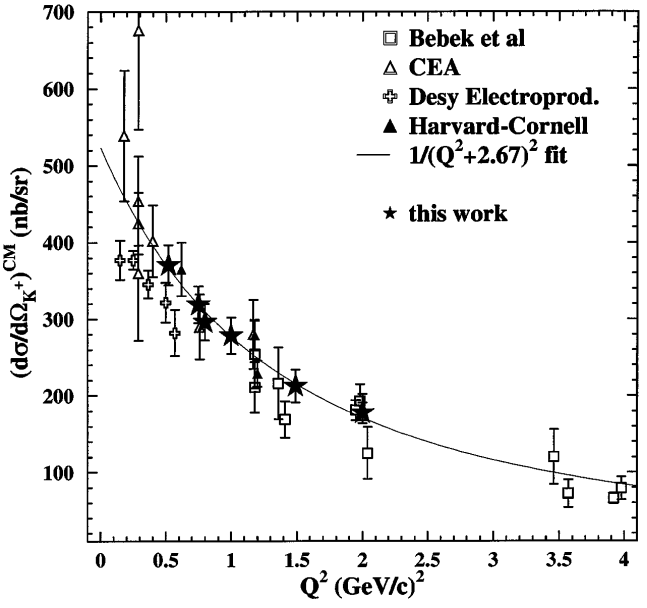

FIG. 3. Summary of the world center-of-mass cross section data for the $e + p \rightarrow e' + K^+ + \Lambda$ reaction. All data are scaled to the same $W = 2.15$ GeV as explained in Ref. [10]. An eye-guiding, simple dipole fit to our unseparated data is also provided.

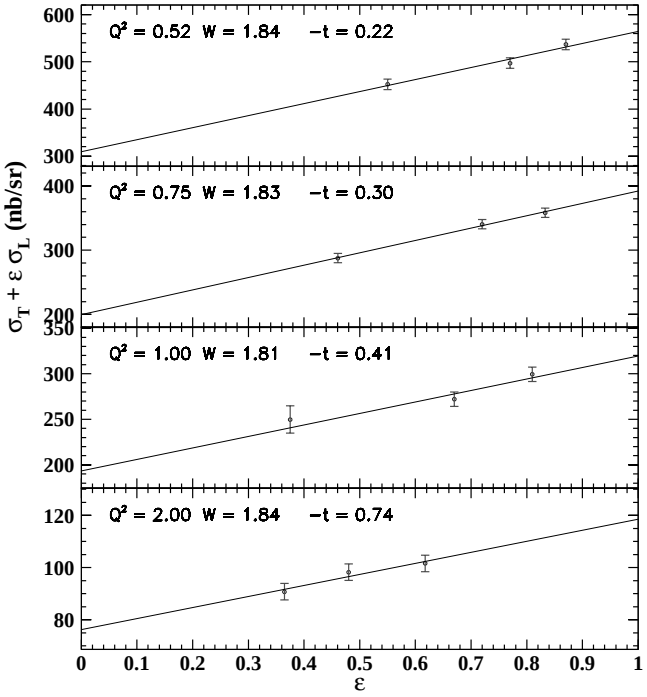

FIG. 4. Unseparated $\sigma_T + \varepsilon\sigma_L$ cross section as a function of the virtual photon polarization ε for different values of squared four-momentum transfer, Q^2. The error bars represent the point-to-point uncertainties (2.1–3.0)% added in quadrature to the statistical uncertainties (0.8–2.0)%. Additionally there is a scale uncertainty of ~5%. The lines represent the best least-squares fit for σ_T and σ_L. The units used are GeV for energy and (GeV/c) for momenta.

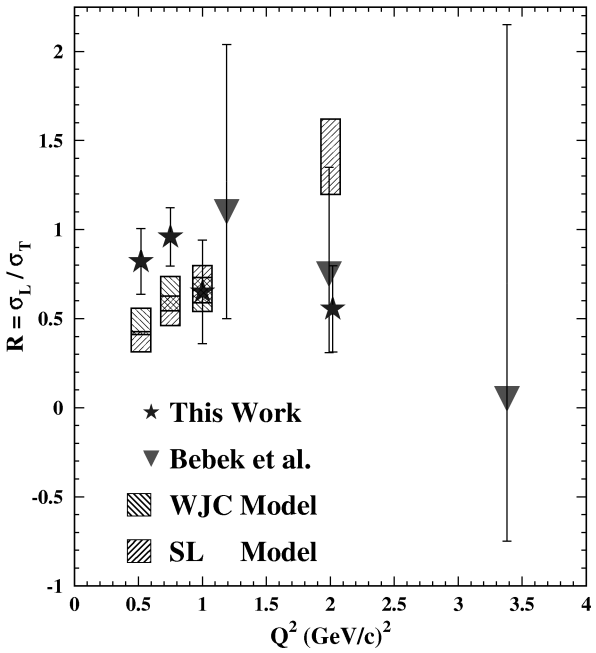

FIG. 5. The ratio $R \equiv \sigma_L/\sigma_T$ as extracted from these data and Ref. [5]. This is the world's complete set of data for the $^1\mathrm{H}(e,e'K^+)\Lambda$ reaction. The calculations are as outlined in Refs. [4,11]. At $Q^2 = 2.0$ (GeV/c)^2, the WJC prediction for R is ~3.5 (off scale).

are in good agreement with the existing world data set. The present data demonstrate the ability to separate the longitudinal and transverse cross sections with a precision significantly greater (~3 times) than the only prior measurement. The data exhibit a strong contribution from the longitudinal part of the cross section, but this contribution is much less than model predictions for the $Q^2 = 2.0$ (GeV/c)^2 point. Current calculations predict that R increases with Q^2 whereas our data support a flat behavior in this kinematic range. The precision of the separated cross sections should serve to constrain and refine theoretical models of associated strangeness production.

TABLE I. Separated transverse and longitudinal cross-sections (and their uncertainties) for the $^1\mathrm{H}(e,e'K^+)\Lambda$ process as measured in experiment E93-018. The quoted uncertainty is the sum in quadrature of all known sources of uncertainties: point-to-point, scale, and statistical.

Q^2 (GeV/c)^2	σ_T [nb/sr]	σ_L [nb/sr]	R
0.52	309.6 ± 39.0	254.6 ± 50.2	0.82 ± 0.18
0.75	199.9 ± 21.2	192.0 ± 29.0	0.96 ± 0.16
1.00	193.4 ± 38.3	125.9 ± 51.2	0.65 ± 0.29
2.00	76.2 ± 9.6	42.4 ± 18.0	0.56 ± 0.24

The authors acknowledge the support of the staff of the Accelerator Division of Thomas Jefferson National Accelerator Facility. This work was supported in part by the U.S. Department of Energy, Nuclear Physics Division, the National Science Foundation, Stichting voor Fundamenteel Onderzoek der Materie (FOM) (Netherlands), and the Korean Science and Engineering Foundation (KOSEF).

[1] Z. Li, Phys. Rev. C **52**, 1648 (1995); C. Bennhold, Nucl. Phys. **A547**, 79c (1992); R. A. Adelseck and L. E. Wright, Phys. Rev. C **38**, 1965 (1988).
[2] C. Bennhold and L. E. Wright, Phys. Rev. C **36**, 438 (1987); S. R. Cotanch and S. S. Hsiao, Nucl. Phys. **A450**, 419c (1986); O. Dumbrajs *et al.*, Nucl. Phys. **B216**, 277 (1983).
[3] R. A. Schumacher, Nucl. Phys. **63c** A585 (1995).
[4] R. A. Williams, C. R. Ji, and S. R. Cotanch, Phys. Rev. C **46**, 1617 (1992).
[5] C. J. Bebek *et al.*, Phys. Rev. D **15**, 3082 (1977).
[6] R. C. Walker *et al.*, Phys. Rev. D **49**, 5671 (1994).
[7] R. C. E. Devenish and D. H. Lyth, Phys. Rev. D **5**, 47 (1972).
[8] C. N. Brown *et al.*, Phys. Rev. Lett. **28**, 1086 (1972).
[9] P. Brauel *et al.*, Z. Phys. C **3**, 101 (1979).
[10] C. J. Bebek *et al.*, Phys. Rev. D **15**, 594 (1977).
[11] J. C. David *et al.*, Phys. Rev. C **53**, 2613 (1996); B. Saghai (private communication).